

Supporting Information

Solvent- and catalyst-free synthesis of an azine-linked covalent organic framework and the induced tautomerization in the adsorption of U(VI) and Hg(II)

Xing Li^{a,‡}, Yue Qi^{b,‡}, Guozong Yue^c, Qianxun Wu^d, Yang Li^a, Meicheng Zhang^a, Xinghua Guo^a, Xiaofeng Li^a, Lijian Ma^{a*} and Shoujian Li^{a*}

a. College of Chemistry, Sichuan University, Key Laboratory of Radiation Physics & Technology, Ministry of Education, Chengdu 610064, P. R. China. E-mail: ma.lj@hotmail.com; sjli000616@scu.edu.cn. Tel.: +86-28-85412329 Fax: +86-28-85412907.

b. Testing & Analysis Center of College of Chemistry, Sichuan University, 29 Wangjiang Road, Chengdu 610064, P. R. China

c. Institute of Materials, China Academy of Engineering Physics, Jianguo 621908, P. R. China.

d. Sichuan University-Pittsburgh Institute, Sichuan University, Chengdu 610207, P. R. China.

[‡]These authors contributed equally to this work.

Table of contents

Table S1 Compositions of the simulated nuclear industrial effluent -----	3
Fig. S1 Raman spectrum of ACOF -----	4
Fig. S2 XPS survey spectra of ACOF (red) and ACOF-U (blue)-----	4
Fig. S3 The comparison of XRD patterns of solv-ACOF and solv-free-ACOF -----	5
Fig. S4 SEM and TEM images of solv-free-ACOF and solv-ACOF -----	6
Fig. S5 The effect of t on the adsorptions of U(VI) onto solv-free-ACOF and solv-ACOF -----	7
Fig. S6 The XPS spectra of the samples after being soaked in pH = 7 (a and b) and pH = 1.5 (c and d) aqueous solution -----	8
Fig. S7 The structure, FT-IR spectrum and XRD pattern of ACOF-TFPB-----	8
Fig. S8 The comparison of effect of pH on the adsorption of U(VI) onto ACOF-TFPB and ACOF-----	9

Table S1 Compositions of the simulated nuclear industrial effluent.

Coexistent ion	Added as	Reagent purity	C_{θ} -calculated (mmol/L)	C_{θ} - measured (mmol/L)
UO₂²⁺	UO ₂ (NO ₃) ₂ ·6H ₂ O	Standard reagent	10	9.70
La³⁺	La(NO ₃) ₃ ·6H ₂ O	99.9% metal basis	10	8.35
Ce³⁺	Ce(NO ₃) ₃ ·6H ₂ O	99.9% metal basis	10	7.96
Nd³⁺	Nd(NO ₃) ₃ ·6H ₂ O	AR	10	8.30
Sm³⁺	Sm(NO ₃) ₃ ·6H ₂ O	AR	10	8.61
Gd³⁺	Gd(NO ₃) ₃ ·6H ₂ O	AR	10	8.38
Mn²⁺	MnO	99.5%	10	7.57
Co²⁺	Co(NO ₃) ₂ ·6H ₂ O	99.9% metal basis	10	8.33
Ni²⁺	Ni(NO ₃) ₂ ·6H ₂ O	Spectrum pure	10	8.09
Zn²⁺	Zn(NO ₃) ₂ ·6H ₂ O	99.9% metal basis	10	8.39
Ba²⁺	Ba(NO ₃) ₂	99.999%	10	8.38

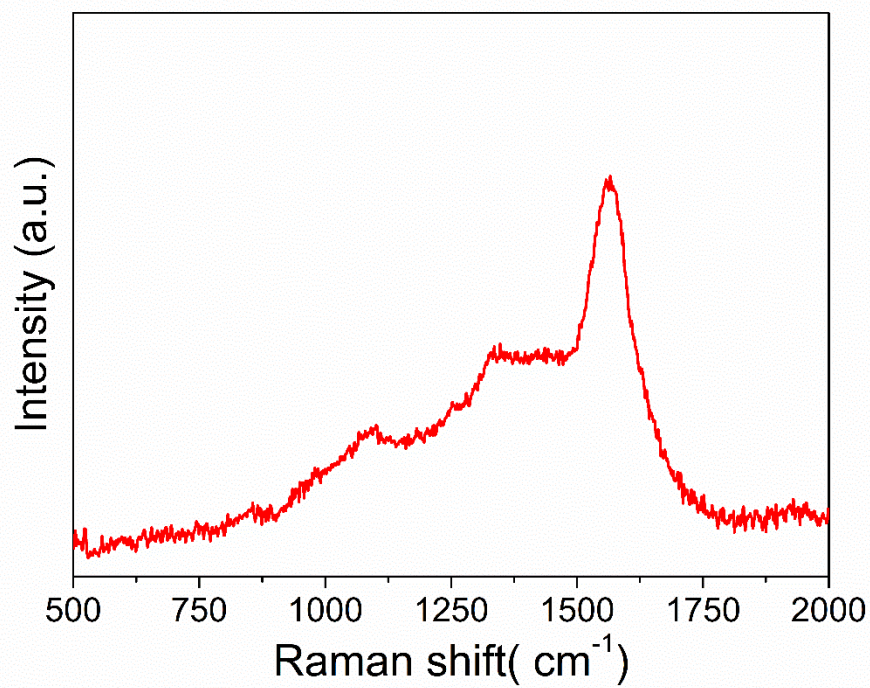


Fig. S1 Raman spectrum of ACOF.

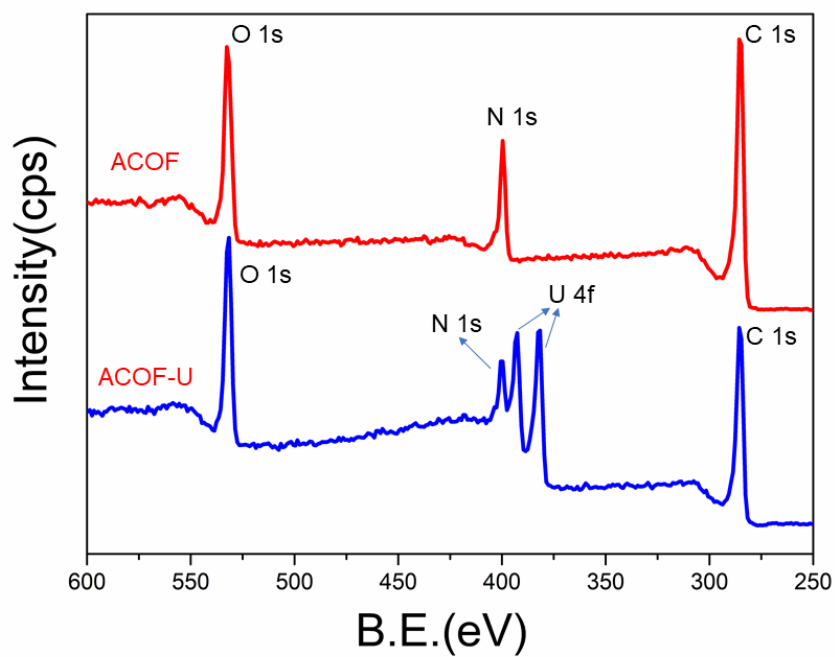


Fig. S2 XPS survey spectra of ACOF (red) and ACOF-U (blue).

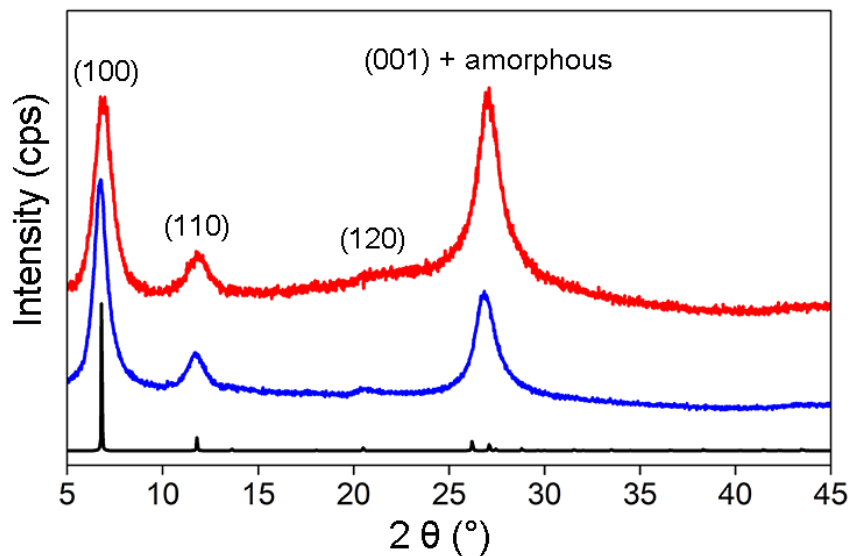


Fig. S3 The comparison of XRD patterns of solv-ACOF (red) and solv-free-ACOF (blue).

The XRD spectrum of solv-ACOF is worse than that of solv-free-ACOF, indicating the better crystallinity of solv-free-ACOF (Compared with the peaks of solv-free-ACOF, the obviously stronger peak of solv-ACOF at 26.80° , the higher baseline and the indistinguishable peak at 20.47° suggest that solv-ACOF contains more amorphous components).

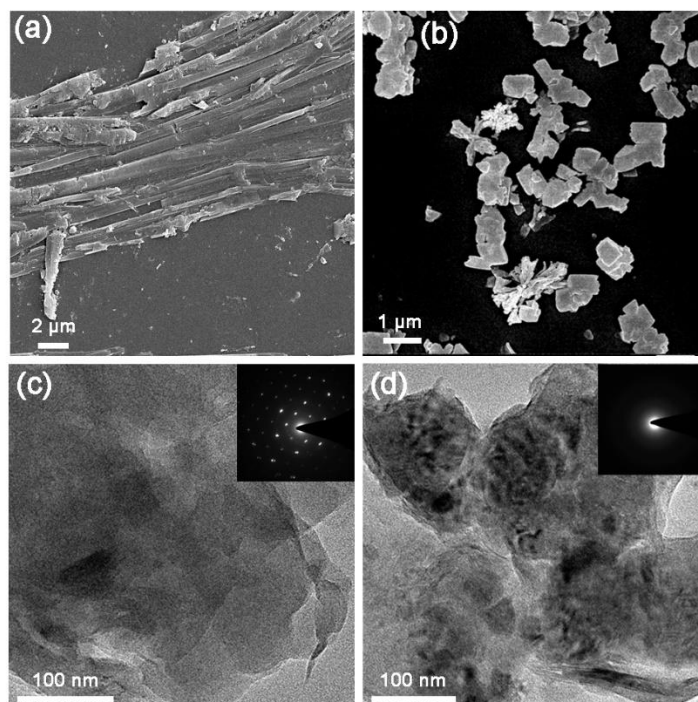


Fig. S4 SEM images of solv-free-ACOF (a) and solv-ACOF (b); TEM images of solv-free-ACOF (c) and solv-ACOF(d) (inset: selected-area electron diffraction patterns).

As can be seen from SEM and TEM images, solv-free-ACOF exhibits lamella in narrow strips in microscope. While solv-ACOF turns out to be irregular bulk with some aggregate structure in the SEM image. What's more, the selected-area diffraction patterns (insets) prove again that the crystallinity of solv-free-ACOF is better than that of solv-ACOF.

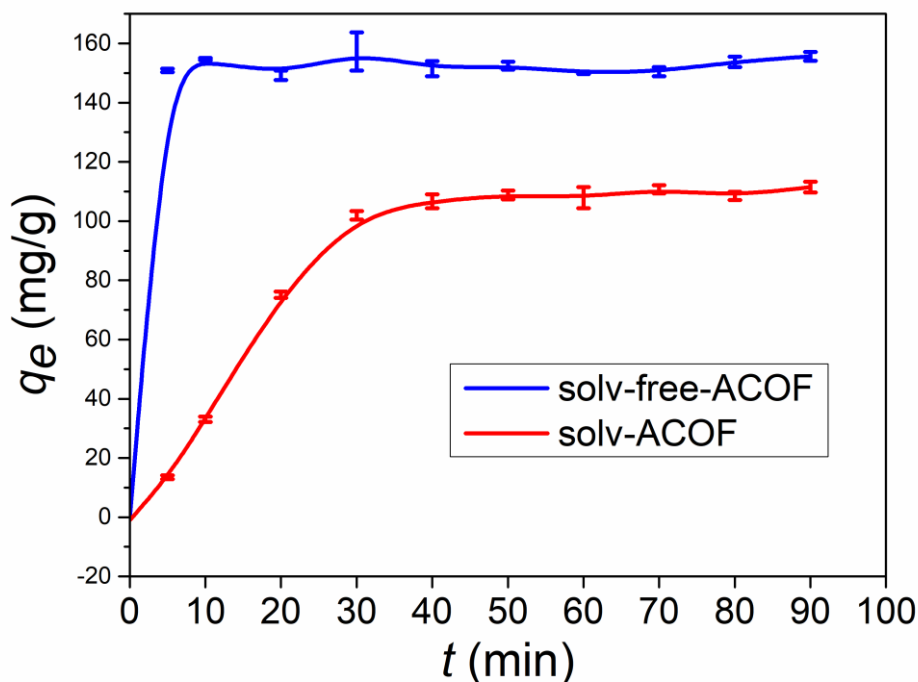


Fig. S5 The effect of contact time (t) for the adsorptions of U(VI) onto solv-free-ACOF and solv-ACOF. ($c_0 \approx 0.5$ mmol/L, $T = 25^\circ \text{C}$, $m = 10$ mg, $V = 25$ mL, $\text{pH} = 4.5$)

As can be seen, the equilibrium adsorption capacity of solv-ACOF is only 118 mg/g, and it takes 30 min to reach the equilibrium. In contrast, the maximum adsorption capacity of solv-free-ACOF is 155 mg/g, and it takes only 5 min to reach the adsorption equilibrium. This could be ascribed to the inadequate exposure of active sites in the amorphous part of solv-ACOF, which leads to the inconvenient contact of U(VI) and active sites, and the irregular microscopic pores and channels in solv-ACOF are not beneficial for the quick combination and diffusion of uranyl ions in the material. Similar phenomena and conclusions have also been described in the literature [Adv. Mater. 2018, 30, 1705479].

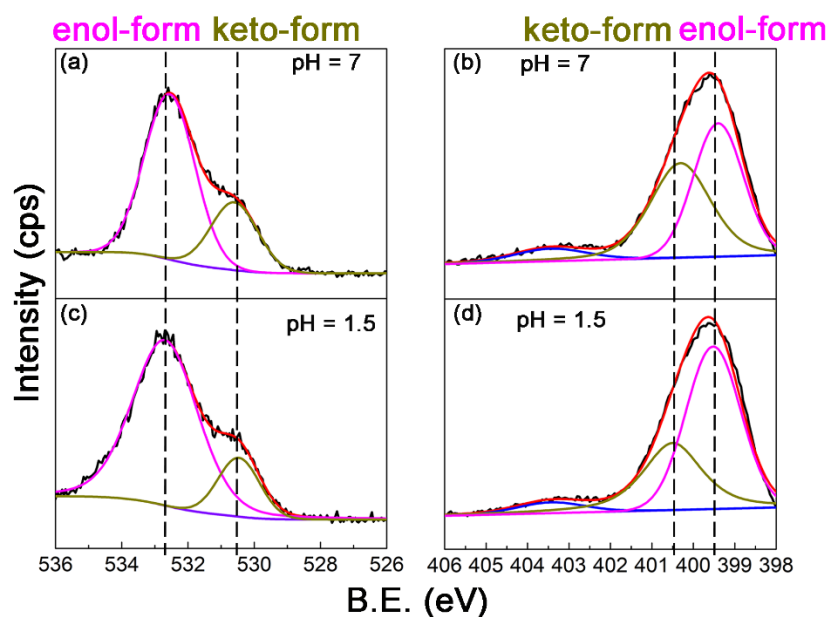


Fig. S6 The XPS spectra of the samples after being soaked in pH = 7 (a and b) and pH = 1.5 (c and d) aqueous solution.

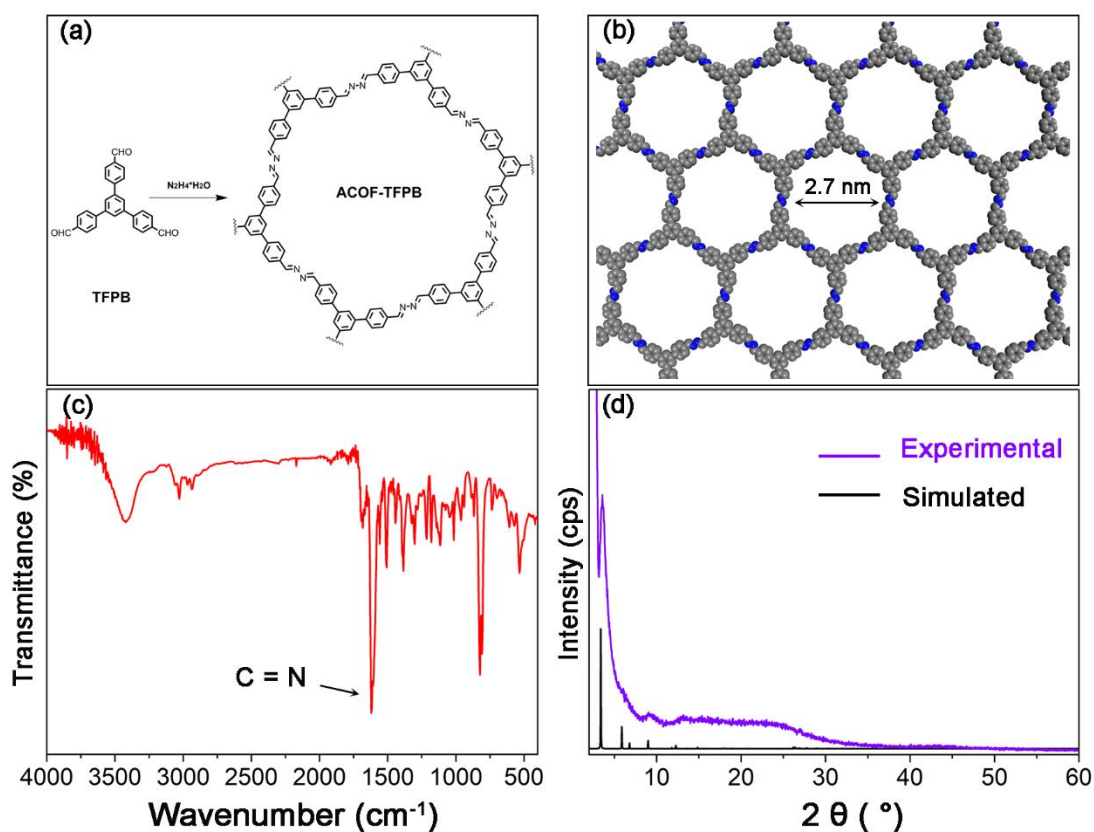


Fig. S7 (a) and (b) the structure of ACOF-TFPB; (c) the FT-IR spectrum of ACOF-TFPB; (d) the experimental and simulated XRD spectra of ACOF-TFPB.

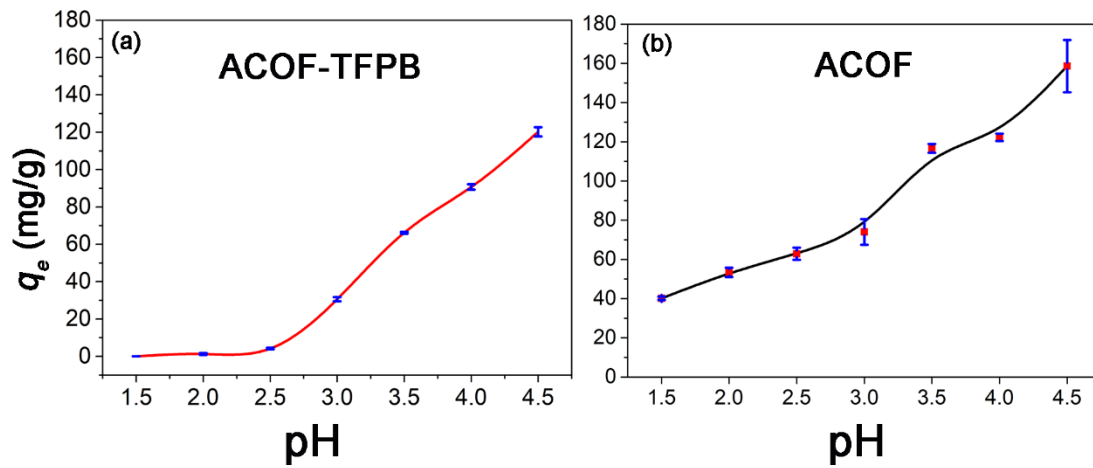


Fig. 8 The comparison of effect of pH on the adsorption of U(VI) onto ACOF-TFPB (a) and ACOF (b). ($c_0 \approx 0.5$ mmol/L, $T = 25$ ° C, $m = 10$ mg, $V = 25$ mL, $t = 12$ h)